5-2022

Quantification of Dental Fissures Through Occlusal Topography Analysis

Duru Erkan

Quantification of Dental Fissures Through Occlusal Topography Analysis

An Honors Thesis submitted in partial fulfillment of the requirements of Honors Studies in Biology

By

Duru Erkan

Spring 2022

Biology

J. William Fulbright College of Arts and Sciences

The University of Arkansas

Acknowledgements

I would like to thank Dr. Peter Ungar for being an invaluable mentor and research advisor throughout my time at the University of Arkansas. Dr. Ungar has guided me through one of the most rewarding experiences of my academic career, and my project would not have been possible without him.

I would additionally like to thank the Honors College for supporting this project through the Honors College Research Grant.

Table of Contents

Acknowledgements ……....1
Table of Contents ……2
Abstract ……...3
Introduction ……4
Procedures ……...5
Statistical Methods ……..9
Results ……9
Discussion ……10
References ……14
Figures and Tables ……16

Abstract

Narrow, deep, and elaborate dental fissures are widely believed to increase the predisposition of enamel to develop carious lesions as these surfaces are thought to be ideal for cariogenic bacteria to adhere to. Therefore, dentists prescribe sealants as a preventative measure for patients with such fissures to avoid tooth decay. Yet to date, there is no objective data supporting the notion that fissure morphology actually affects caries susceptibility, nor is there a quantifiable, clinically practical method to characterize fissure patterns expected to increase risk of caries disease.

In this study, three new methods to quantitatively characterize fissure pattern in mandibular first molars were developed using widely available 3D analytic software and intraoral scanners newly common in dental clinics. The first method defines fissure pattern through measuring groove-fossa-system angles. The second uses the percent of pixels representing the occlusal surface comprising fissures. Lastly, the third focuses on fissure surface area difference. Using these methods, fissure attributes were compared with caries progression data of the 166 specimens to test the hypothesis that deeper, more voluminous fissures would lead to caries and cavity progression.

Results illustrate that the three methods developed measure different but complementary aspects of fissure pattern, offering a more robust characterization than previously achieved by other methods. I envision that combining the methods I created, a software package for intraoral scanners can be generated to allow for quick and reliable examination of fissures in clinics and research labs. However, the hypothesis that fissure pattern, as characterized in this study, affects susceptibility to caries was rejected for this dataset as no significant association between the two was found. Considering the limitations of this analysis, future studies with better control over the sample and more time allotted for caries progression are warranted to confirm that no relationship exists between fissure morphology and caries progression.

Introduction

Occlusal surface morphology is believed to affect the predisposition of teeth to develop dental caries (Khanna et al., 2015). Therefore, it is especially important for dentists to characterize and monitor the pits and fissures on patients' teeth. Most dentists believe that the narrower and the more intricate fissures are, the more likely plaque bacteria will adhere to the enamel and the harder it is to clean all parts of the surface (König, 1963; Muller-Bolla et al., 2009). When these susceptible areas remain untouched, cariogenic bacteria increase the probability of tooth decay (König, 1963; Muller-Bolla et al., 2009). Dentists therefore "seal" the most cavity-prone parts of patients' teeth to prevent enamel destruction (Deery, 2013). However, the decision to seal is based on intuition and experience during visual examination rather than objective criteria (Courson et al., 2011). Dentists lack quantifiable, clinically practical measures to identify exactly which teeth need sealants and which do not. As a result of limited efforts to quantify fissure attributes, there are also no empirical data supporting the notion that fissure morphology actually affects caries susceptibility. Consequently, sealants may be systematically overused, causing some patients unnecessary expense (Courson et al., 2011; Deery, 2013).

Until now, there have been few attempts to develop qualitative characterizations of fissure pattern and even fewer efforts to develop quantitative ones (Fusayama & Kurosu, 1964; Awazawa, 1969). Most qualitative measures make use of 2D visual analysis through microscopy and x-ray scanning, which do not adequately characterize the three-dimensional aspect of fissure patterns (Arhatari et al., 2014; Khanna et al., 2015). Others are either impractical in a clinical setting or too invasive (Nagano, 1961; Juhl, 1983). Three-dimensional analysis for this purpose has been left largely unexplored.

One notable quantitative method is the morphometric analysis of two-dimensional groove-fossa-system surface profiles developed by Ekstrand, Carlsen, and Thylstrup (1991). Ekstrand et al. (1991) found that it is possible to describe the two-dimensional profile of fissures by groove depth and angle. They extracted and serially sectioned teeth in right angles to the mesiodistal axis of the crown. Then, two lines were drawn from the deepest point of the section to the highest point on the lingual and buccal cusps. These lines were sectioned into thirds, and perpendiculars were raised from the sections closest

to the base to the sides of the cusps. Additional lines were drawn from the base to meet these intersections along section outlines, and the angle between the final set of lines was measured (Ekstrand et al., 1991) (Fig. 1).

While this method achieves a quantitative classification of fissure complexity through angle measurement, it cannot be used in a clinical setting as it requires extraction and sectioning of the tooth. Therefore, dentists have preferred a brief, qualitative, and subjective visual examination of fissures to recommend sealants instead.

The goal of this study was to explore new methodology for rapid, inexpensive, and repeatable fissure quantification using widely available 3D analytic software and newly available intraoral scanners that are becoming common in dental clinics today. An effective fissure classification method could test the hypothesis that fissure morphology affects susceptibly to caries and help dentists recommend sealants objectively. It could also be a useful tool for future research endeavors relating to occlusal morphology.

In this study, three different fissure attribute quantification methods were developed using digital elevation models of 166 mandibular first molars. The first method quantifies fissures based on the angle they create with cusps similar to the method developed by Ekstrand et al. (1991). The second uses the percent of pixels representing the occlusal surface comprising fissures. Lastly, the third focuses on fissure surface area. Data obtained from the three novel methods were tested in relation to the molars' clinical caries progression data. I hypothesized that these three attributes would yield complementary characterizations, and that surfaces with deeper, more voluminous fissures would be more likely to develop cavities, per popular conviction.

Procedures

Specimens used to develop fissure quantification methods were acquired from a previous study (Sarah Buedel's master's thesis study titled "Quantitative Evaluation of Dental Occlusal Topography for Caries Prediction of Orthodontic Patients," 2020). Digital elevation models of 192 erupted, left and right permanent mandibular first molars from de-identified orthodontic patients at the Indiana University School of Dentistry were used after study protocol review and approval by the local Institutional Review Board (process #1908412111). Each molar was treated independently. Two models were

obtained per specimen, one taken pre-orthodontic treatment and one post-treatment, approximately two years apart. The digital scans were taken using a Carestream 3600 (Carestream Dental, Atlanta, GA) intraoral scanner and retrieved from the Dolphin Imaging (Dolphin Imaging and Management Solutions, Chatsworth, CA) archive of comprehensive orthodontic treatment records. The scans were selected based on completeness of eruption, scan quality, comprehensiveness of dental records, and absence of any previous restorations extending to the molar's occlusal surface. Age, gender, race, and/or ethnicity were not used as inclusion/exclusion criteria. Of the original 192 scans examined, only 166 were used for the study as some specimen were discarded due to artifacts in the fissure system or scanning errors.

Caries Identifiers

The specimens were ranked for caries incidence through x-ray analysis by board-certified dentists at the Indiana University School of Dentistry using the ICDAS—International Caries Detection and Assessment System—during the initial and final examinations for orthodontic treatment, approximately two years apart. The ICDAS classifies caries on a scale of 0—a sound tooth—to 6—a tooth with advanced carious lesions. However, the most severe lesion observed in our sample was a rating of 5. While some teeth developed caries and their ICDAS ranking increased from the first scan to the last, others did not. In addition, some teeth had undergone restoration or had been sealed due to advanced cavity development in the final round of scanning. Those specimens were not ranked on the number scale, but rather noted as either restored or sealed. The ICDAS data from the initial and final scans were then compared, and caries progression rated as YES-there is progress, NO-there is no progress, and UNKNOWN-for teeth that had undergone restoration or sealants.

Quantification of Fissure Attributes

In order to retain consistency in the analysis of fissure attributes, I aligned, oriented, and cropped the intraoral 3D digital scans of the molars following the procedure developed by Alwadi et al. (2020). Tooth scans (.PLY format) were imported into MeshLab, a 3D mesh processing software system. Using the tools available in MeshLab,

the molars were isolated individually, and oriented on an x-y-z coordinate system. The specimens were aligned to be vertically intersected by the z-axis, erupting in the positive-z direction. The teeth were further oriented to where the highest crest was closest to the y axis with the x axis running along its depth, and the tooth positioned in the positive x-y quadrant. Then, the scans were vertically aligned so that the y-axis cut through the midpoint of the cervix on the long side of the tooth, and the x-axis cut through the midpoint of the cervix on the short side (Fig. 2). The oriented scans were saved and opened in Geomagic Wrap, a 3D image processing and analysis software package, to isolate occlusal surfaces. The scans were cropped using an x-y plane parallel to the cementoenamel junction at the lowest point on the central basin. Tooth structures below the cropping plane were removed to leave behind the occlusal table (Fig. 3). The final modified scans were used in the development and testing of the three fissure quantification methods.

Method 1: Average Fissure Angles

I developed a digital version of Ekstrand et al. (1991)'s method as a non-invasive alternative to measure fissure angles by sectioning teeth. To obtain the best view and angle of the fissures, a line can be drawn from the tip of the anterior buccal cusp (protoconid) to that of the anterior lingual cusp across from it (metaconid), and the tooth scan can be cropped at this line using Geomagic Wrap. The same can be done for the posterior cusps (hypoconid to entoconid). However, in order to standardize the section lines and take into account teeth with excessive wear and therefore no visible "cusp tip," cusp midpoints were used instead to produce section lines in this study.

Tooth cusps can be thought of as irregular hemispheres. Accordingly, the protoconid, metaconid, entoconid, and hypoconid on each of the specimens were traced out and fit into spheres using the Feature Detection Tool on Geomagic Wrap (Fig. 4a). The midpoints of these spheres were found and used as markers for the ends of section lines (Fig. 4b). Opposing cusps were connected at these midpoints, and the produced line was used to section the teeth (Fig. 4c and Fig. 4d). The fissures were viewed by looking into the molars mesiodistally (Fig. 5). Two-dimensional screen captures were taken of these sections (.JPG format), and the images were imported into Adobe Photoshop to

measure the fissure angles as described by Ekstrand et al. (1991) (see Introduction and Fig. 1). The angle measured from the protoconid-metaconid section and the angle from the hypoconid-entoconid section were averaged to obtain one angle value per specimen.

Method 2: Percent of Fissure Pixels

The digital elevation models were opened with Geomagic Wrap (.PLY format), and a contour map was laid on top of each surface. The contour map color codes each mesh triangle on the basis of elevation and angle. Flat surfaces are coded as blue/green, and surfaces with pronounced angles are coded as yellow/red by default through the Geomagic algorithm (Fig. 6). Screen captures of the contoured occlusal surfaces were taken (.JPG format), and these images were imported onto Adobe Photoshop. The teeth were cropped with the Magnetic Lasso Tool to exclude their backgrounds. The number of yellow/red pixels on each tooth was computed with the Histogram algorithm. This value was divided by the total number of pixels in the occlusal table of each tooth to calculate the percent of fissures that make up the surface area. Consistent and repeatable measures were produced due to the standardization of algorithms used.

Some teeth had landmarks, such as pits at cusp tips due to wear, that were not a part of the main fissure system. In order to prevent these landmarks from being counted in the percent fissure area, the artifacts were covered with green/blue paint using the Brush tool. This way, a precise and repeatable measurement of percent of fissure pixels was obtained.

Method 3: Fissure Surface Area Difference

The tooth scans were opened in Geomagic Wrap (.PLY format), and their raw surface areas were computed. Then, using the Relax Polygons algorithm, the teeth were smoothed to maximum smoothness by full strength with minimum curvature priority (Fig. 7). This action minimized the pits and fissures on the occlusal surfaces. Surface areas were calculated once again, and the original areas were divided by the smoothed areas to get relative difference measures of the fissures. The tolerances for the relax polygon algorithm were consistent, and the results were therefore repeatable and comparable between specimens.

Statistical Methods

A Multivariate Analysis of Variance (MANOVA) model was used to determine whether caries development varied in a predictive way with the three fissure attributes quantified. Dependent variables included average fissure angle, percent of fissure pixels, and fissure surface area difference. Caries identifiers were tested as independent variables. The data were ranked and transformed for statistical testing to mitigate violation of assumptions inherent to parametric statistical tests (Conover & Iman, 1981). The first MANOVA test was used to determine whether there were differences in fissure attributes between samples parsed by presence/absence of caries at the initial examination. Using the initial ICDAS data, specimens with an ICDAS ranking of 0 were coded as NO-caries absent, and specimens with a score of 1 and higher were coded as YES-caries present. The second MANOVA test observed the relationship between caries progression from initial scanning to final scanning and variation in the three attributes. Caries progression was identified as YES-there is progress, NO-there is no progress, and UNKNOWN-for teeth that had undergone restoration or sealants (see the "Caries Identifiers" section in Procedures). The third test looked at the association between initial ICDAS score (considering each number on the range) and variation in fissure attributes. Finally, the fourth examined the association between ICDAS score at the final scanning (considering each number on the range) and variation in fissure pattern.

A second set of tests were performed using pair-wise Spearman's non-parametric Rank Order Correlation in order to determine whether the three fissure attributes were correlated with one another.

Results

We observed that none of the three attributes measured are significantly associated with caries. The first MANOVA test illustrated that there are no statistically significant differences in fissure pattern (as characterized by the three quantifiable attributes) based on the presence or absence of caries (Table 1 and Fig. 8). The second MANOVA test demonstrated that there are no statistically significant differences in fissure pattern based on caries progression (Table 2 and Fig. 9). The results of the third MANOVA test further indicated that there are no statistically significant differences in

fissure pattern based on initial ICDAS score (Table 3 and Fig. 10). Lastly, the fourth MANOVA test revealed no statistically significant differences in fissure attributes based on final ICDAS score (Table 4 and Fig. 11).

The pair-wise Spearman's non-parametric Rank Order Correlations demonstrated that all three fissure attributes are significantly correlated with one another (Table 5 and Fig. 12). The results of Spearman's Correlation Test for average fissure angle and percent of fissure pixels indicated that there is a statistically significant correlation between the two variables, n=166, r_s=0.341 ($p < .00001$). We also found that there was a statistically significant correlation between percent of fissure pixels and fissure area difference, n=166, r_s=-0.267 (p=.000506). Lastly, we observed a statistically significant correlation between fissure area difference and average fissure angle as well, n=166, r_s=0.220 (p= 0.004399). Nevertheless, the spread of points is substantive, and r_s values are low, suggesting that the significance is likely driven, at least in part, by the relatively large sample size. From Figure 12, it is clear that it would be difficult to predict one aspect of fissure pattern from another.

Discussion

The primary goal of this study was to develop new methods to quantitatively characterize fissure pattern in human mandibular first molars using widely available 3D analytic software and intraoral scanners newly common in dental clinics. The significant but low associations between individual attributes suggests that the methods describe different but complementary information about fissure pattern. These together seem to offer a more robust characterization of fissure pattern than has been previously achieved using other techniques.

Digitally computing fissure angles as described by Ekstrand et al. (1991) provides a measure of fissure breadth and slope. The precision of this method can be seen visually in Figure 1. The drawn lines evidently represent an accurate measure of the fissure angle in cross-section. Percent of fissure pixels also appears to be a fitting attribute to quantify extent of fissures across the surface. As can be seen on Figure 6b, the algorithm that codes each mesh triangle via slope and elevation is precise and consistent. Thus, computing the percent of red/yellow pixels that make up an occlusal surface gives a

reliable description of fissure area. Lastly, fissure surface area difference provides a volumetric characterization of the proportion of fissures that make up an occlusal table. These three methods look at different aspects of fissure form, and together seem to give a fairly complete picture of fissure morphology and extent.

All three methods are non-invasive, cost-effective, and rapid in nature. Intraoral scanning equipment is becoming relatively inexpensive and increasingly common for digital molding in the dental industry. Dentists can obtain three-dimensional scans of patients' teeth within minutes using these scanners. Examining fissures for caries prevention through three-dimensional scanning could be an additional benefit to preventative dental practice. Using equipment already available in clinics for fissure inspection could be a cost-effective way to monitor cavity progression.

Furthermore, including the cropping and aligning process, each individual method I developed takes around 5-10 minutes to produce a final value. Although Geomagic Wrap, MeshLab, and Adobe Photoshop could easily be used in future research endeavors looking to quantify occlusal fissures, these packages will likely never be used in dental clinics. However, specialized software with similar algorithms can be developed to accomplish the same characterizations. The methods I developed were used as a proof of concept; I found that it is possible to quantitatively characterize fissures using different pattern attributes. I envision that a software can be created, perhaps as an add-on module to another existing software package offered by intraoral scanning companies, that combines the methods I created and allows for a quick yet reliable examination of fissures for cavity progression. For these reasons and the robust characterization of fissures the three methods provide, I conclude that the proposed methods could be useful to survey fissures for different purposes.

Although I was able to successfully develop complementary fissure quantification methods as described by different fissure attributes, our hypothesis that surfaces with deeper, more complex fissures would be more likely to develop cavities was rejected. Variations in the three fissure attributes were not significantly correlated with any of the caries identifiers. Although the results of the MANOVA tests relating to initial and final ICDAS scores were close to significant (as close as $p=0.052$), none of the four tests provided a Wilk's Lambda with a p-value less than 0.05. While these results may suggest

inadequate characterization of form to detect susceptibility to caries, this seems unlikely given the number of different methods used and their capture of shape and formation. It can unmistakably be seen that the methods developed were fitting to describe fissure pattern from the figures and statistics provided. It is more likely that either fissure shape does not affect susceptibility to caries (as has previously been concluded by Buedel (2020)) or that the studied sample was inadequate to detect caries susceptibility. The study conducted by Buedel (2020) determined that 3D quantitative occlusal topographical parameters were not associated with caries progression. While Buedel (2020) looked at the entire occlusal surface of specimens to predict caries disease, per her recommendation for follow-up studies, only pit and fissure morphology was considered in my study. Yet I still found no association between caries development and fissure variation. These results suggest that it may be beneficial to conduct another follow-up study with more control over the population since caries can be caused by a combination of various environmental and genetic factors (Fontana & Zero, 2006; Evans et al., 2008). In addition, greater time between initial and final examinations and a larger sample of molars could also be helpful.

Caries differ in their development trajectory depending on lesion severity (Pitts, 1983; Shwartz et al., 1984; Foster, 1998). Zandona et al. (2012) states that as lesion severity increases, the time it takes to progress to cavitation decreases. For example, while an enamel lesion with an ICDAS score of 1 could take up to four years to progress to cavitation, a lesion with a score of 4 is likely to progress in a year (Zandona et al., 2012). Considering that the majority of our sample had low-severity lesions at the initial scoring, a longer time frame could reveal different results.

There are other limitations to this study of notable mention. First, only mandibular fist molars were used in this study. Results may differ with the inclusion of maxillary and second or third molars. A follow up study with a larger, more diverse sample of molars could mitigate any possible bias in our results. Second, the specimens were inspected for caries only though their two-dimensional intraoral photographs. Clinical, direct examination of patients would be ideal to avoid inaccurate scoring of the teeth. Third, variation in the occlusal topography of specimens could have led to discrepancies in our methodology. For example, specimens with complex, hard-to-identify central fissures as

well as those with highly worn surfaces had to be discussed among our group. These complex cases therefore may have introduced uncertainty to the results. Considering these limitations, it is most likely that if a relationship between fissure formation and caries progression exists, the sample was insufficient to detect such a relationship even though the methods developed seemed to be appropriate.

Nevertheless, the findings of this study could indicate that fissure morphology may not be as relevant to caries development as widely believed. It may be that some factors are more highly associated with caries development than fissure pattern, for example diet and hygiene (Fontana & Zero, 2006; Evans et al., 2008). If in the end, fissure anatomy does not turn out to be a significant determinant of caries development, visual assessment of fissures may not be an accurate method of sealant prescription. Future studies are recommended to explore this relationship further.

References

Alwadai, G. S., Roberts, G., Ungar, P.S., González-Cabezas, C., Lippert, F., Diefenderfer, K.E., Eckert, G.J., Hara, A.T. (2020). Monitoring of simulated occlusal tooth wear by objective outcome measures. Journal of Dentistry, 102, 103476.

Arhatari, B. D., Andrewartha, K., & White, M. (2014). Micro X-ray computed tomography of pits and fissures. Journal of X-ray science and technology, 22(4), 407–414. https://doi.org/10.3233/XST-140435

Awazawa, Y. (1969). Re-examination of the morphology of caries susceptible grooves in the premolar and molar. Journal of Nihon University School of Dentistry, 11, 1-15.

Buedel, S. K. (2020). Quantitative Evaluation of Dental Occlusal Fissure System Morphology for Caries Prediction of Orthodontic Patients [Unpublished master's thesis]. Indiana University School of Dentistry.

Conover W.J. & Iman R.L. (1981). Rank transformations as a bridge between parametric and nonparametric statistics. Am Stat 35:124–129. https ://doi.org/10.1080/00031 305.1981.10479 327

Courson, F., Velly, A.M., Droz, D., Lupi-Pégurier, L., & Muller-Bolla, M. (2011). Clinical decision on pit and fissure sealing according to the occlusal morphology. European Journal of Paediatric Dentistry, 12, 43-49.

Deery, C. (2013). Caries detection and diagnosis, sealants, and management of the possibly carious fissure. British Dental Journal, 214, 551-557.

Ekstrand, K. R., Carlsen, O., & Thylstrup, A. (1991). Morphometric analysis of occlusal groove-fossa-system in mandibular third molar. Scandinavian journal of dental research, 99(3), 196–204. https://doi.org/10.1111/j.1600-0722.1991.tb01885.x

Evans, R. W., Pakdaman, A., Dennison, P. J., & Howe, E. L. (2008). The Caries Management System: an evidence-based preventive strategy for dental practitioners. Application for adults. Australian dental journal, 53(1), 83–92. https://doi.org/10.1111/j.1834-7819.2007.00004.x

Fontana, M., & Zero, D. T. (2006). Assessing patients' caries risk. Journal of the American Dental Association (1939), 137(9), 1231–1239. https://doi.org/10.14219/jada.archive.2006.0380

Foster, L. V. (1998). Three year in vivo investigation to determine the progression of approximal primary carious lesions extending into dentine. British dental journal, 185(7), 353–357. https://doi.org/10.1038/sj.bdj.4809812

Fusayama, T. & Kurosu, A. (1964). Diagnosis and distribution of pits and fissures. The Journal of Prosthetic Dentistry, 14, 117-126.

Juhl, M. (1983). Three-dimensional replicas of pit and fissure morphology in human teeth, Scandinavian Journal of Dental Research, 91, 90-95.

Khanna, R., Pandey, R.K., & Singh, N. (2015). Morphology of pits and fissures reviewed through scanning electron microscope. Dentistry, 5. Retrieved from http://dx.doi.org/10.4172/2161-1122.1000287.

König, K.G. (1963). Dental morphology in relation to caries resistance with special reference to fissures as susceptible areas. Journal of Dental Research, 2, 461-476.

Muller-Bolla, M., Courson, F., Droz, D., Lupi-Pégurier, L., & Velly A.M. (2009). Definition of at-risk occlusal surfaces of permanent molars. Journal of Clinical Pediatric Dentistry, 34, 35- 42.

Nagano, T. (1961). Relation between the form of pit fissure and the primary lesion of caries. Dental Abstracts, 6, 426.

Pitts, N.B. (1983). Monitoring of caries progression in permanent and primary posterior approximal enamel by bitewing radiography. Community Dental Oral Epidemiology 11, 228-235.

Shwartz, M., Gröndahl, H. G., Pliskin, J. S., & Boffa, J. (1984). A longitudinal analysis from bite-wing radiographs of the rate of progression of approximal carious lesions through human dental enamel. Archives of oral biology, 29(7), 529–536. https://doi.org/10.1016/0003-9969(84)90074-8

Zandoná, F.A., Santiago, E., Eckert, G. J., Katz, B. P., Pereira de Oliveira, S., Capin, O. R., Mau, M., & Zero, D. T. (2012). The natural history of dental caries lesions: a 4-year observational study. Journal of dental research, 91(9), 841–846. https://doi.org/10.1177/0022034512455030

Figures and Tables

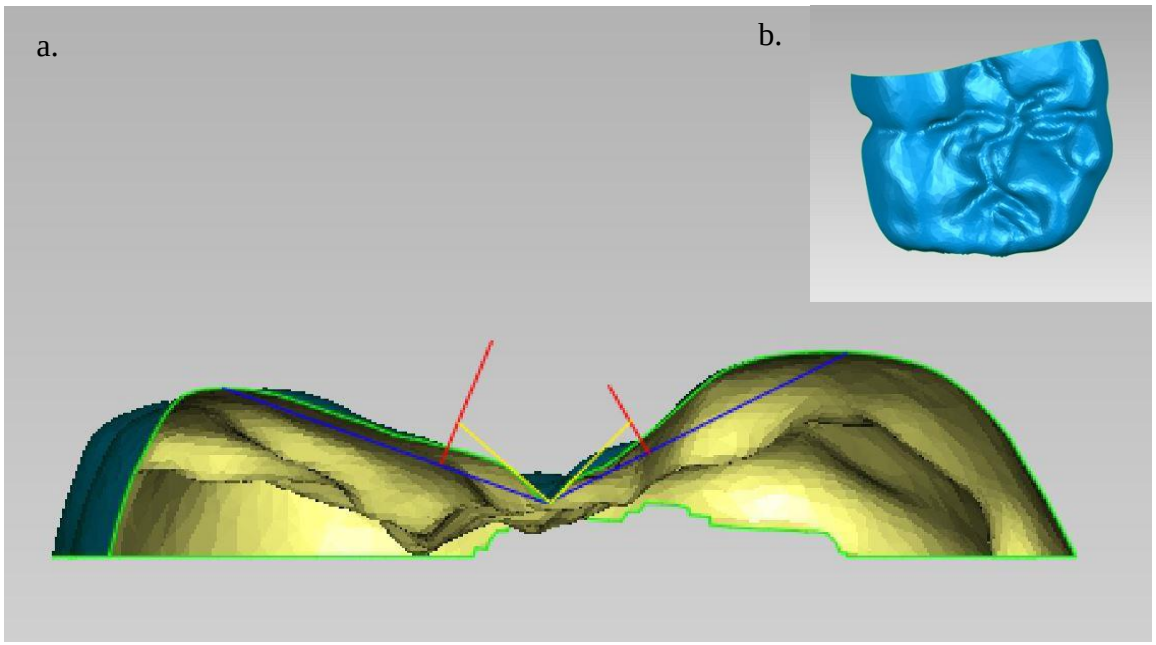

Figure 1 a. Digital representation of Ekstrand et al. (1991)'s method. Two lines are drawn from the central basin to cusp tips (blue). These lines are split into thirds, and the first thirds are used to raise perpendiculars (red). A third set of lines are drawn from the basin to meet the perpendiculars along the tooth section outline (yellow). The angle between the yellow lines is measured. **b.** Occlusal view of the same sectioned tooth.

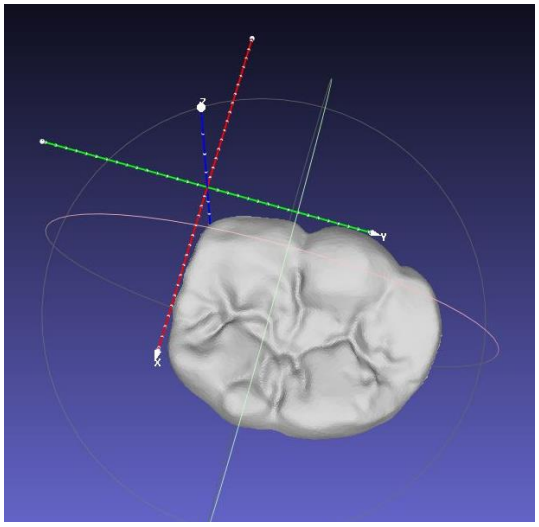

Figure 2. Properly oriented mandibular first molar in MeshLab.

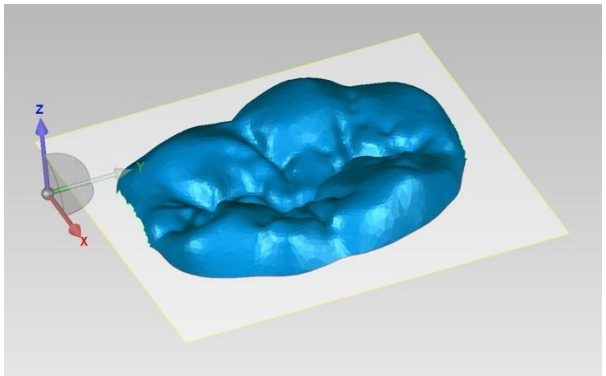

Figure 3. X-Y plane cropped mandibular first molar in Geomagic Wrap.

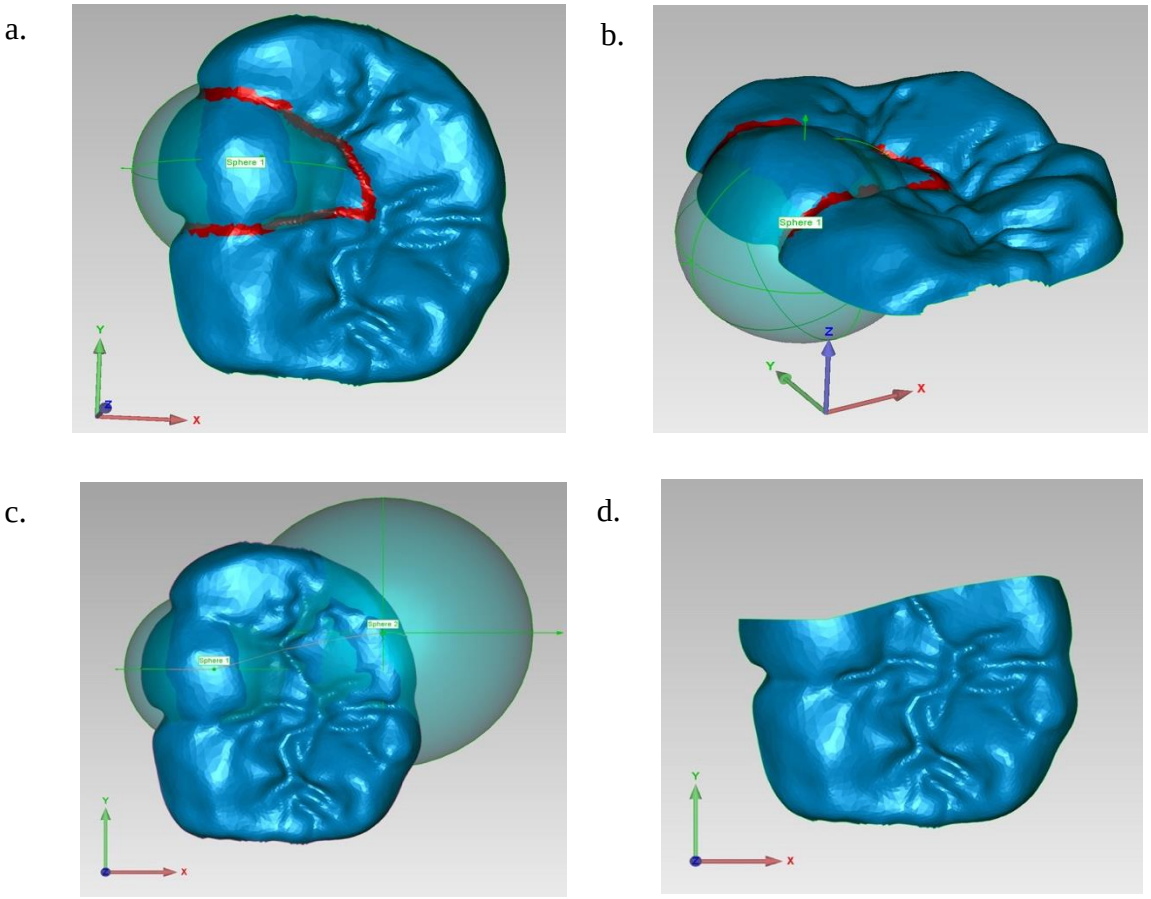

Figure 4 a. Hypoconid of a mandibular first molar traced and fit into a sphere on Geomagic Wrap. **b.** Side view of the sphere fitted cusp. Cusp midpoint is identified by the perpendicular arrow intersecting the hypoconid. **c.** Section line drawn through the hypoconid and entoconid midpoints. **d.** Sectioned molar using the hypoconid-entoconid section line.

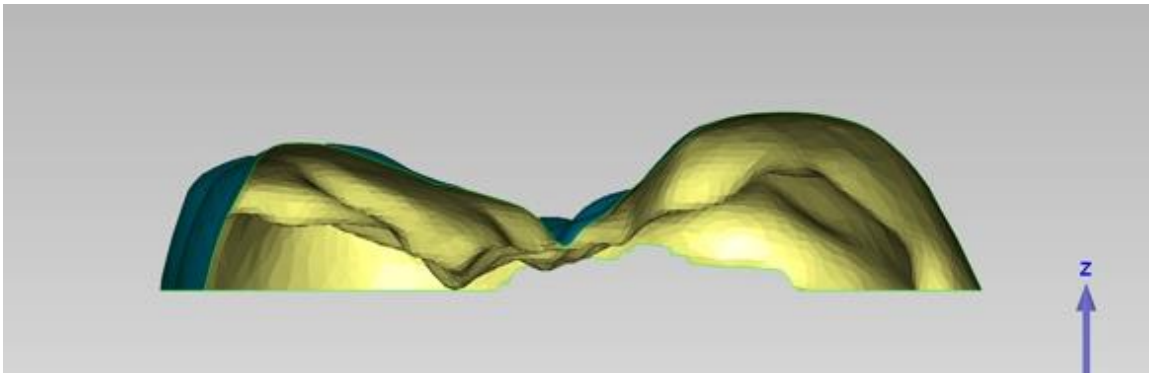

Figure 5. Screen capture of the mesiodistal view of a hypoconid-entoconid sectioned molar.

a. b.

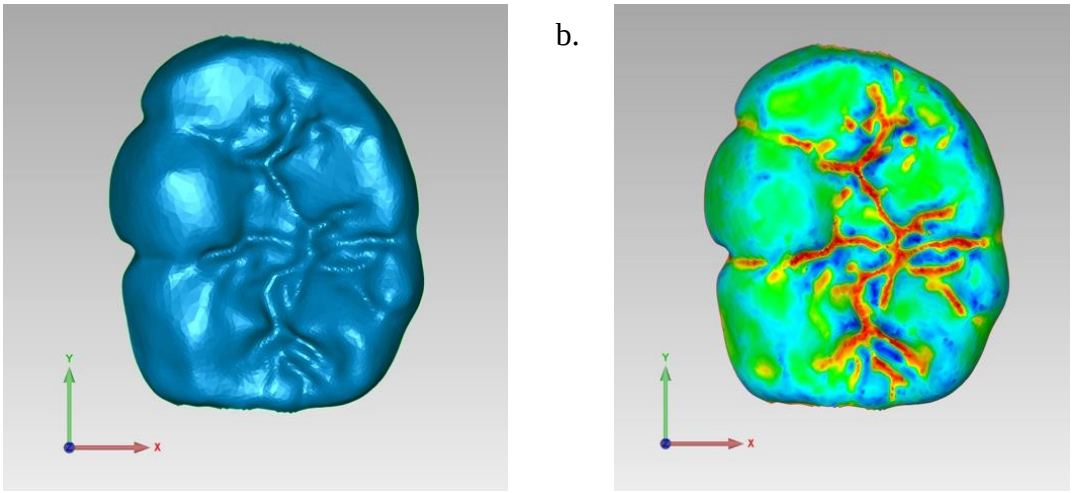

Figure 6 a. Occlusal view of a mandibular first molar. **b.** The same mandibular first molar with a color-coded contour map laid on top.

a. b.

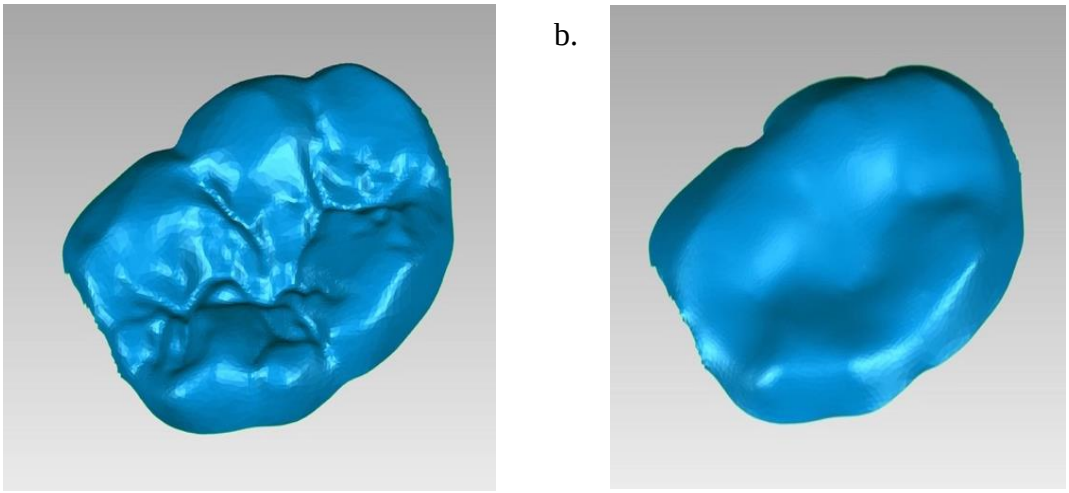

Figure 7. a. Raw mandibular first molar used to calculate the initial occlusal surface area. **b.** The same tooth after smoothing to calculate the surface area without fissures.

Presence/Absence of Caries				
Statistic	Value	F-Ratio	df	p-Value
Wilks's Lambda	0.972	1.547	3, 162	0.204
Pillai Trace	0.028	1.547	3, 162	0.204
Hotelling-Lawley Trace	0.029	1.547	3, 162	0.204

Table 1. MANOVA model observing the variance in initial caries presence or absence with the three attributes measured.

Caries Progress				
Statistic	Value	F-Ratio	df	p-Value
Wilks's Lambda	0.945	1.53	6, 322	0.168
Pillai Trace	0.055	1.533	6, 324	0.167
Hotelling-Lawley Trace	0.057	1.527	6, 320	0.169

Table 2. MANOVA model observing the variance in caries progression with the three attributes measured.

Initial ICDAS				
Statistic	Value	F-Ratio	df	p-Value
Wilks's Lambda	0.957	2.436	3, 162	0.067
Pillai Trace	0.043	2.436	3, 162	0.067
Hotelling-Lawley Trace	0.045	2.436	3, 162	0.067

Table 3. MANOVA model observing the variance in initial ICDAS score with the three attributes measured.

Final ICDAS				
Statistic	Value	F-Ratio	df	p-Value
Wilks's Lambda	0.951	2.637	3, 155	0.052
Pillai Trace	0.049	2.637	3, 155	0.052
Hotelling-Lawley Trace	0.051	2.637	3, 155	0.052

Table 4. MANOVA model observing the variance in final ICDAS score with the three attributes measured.

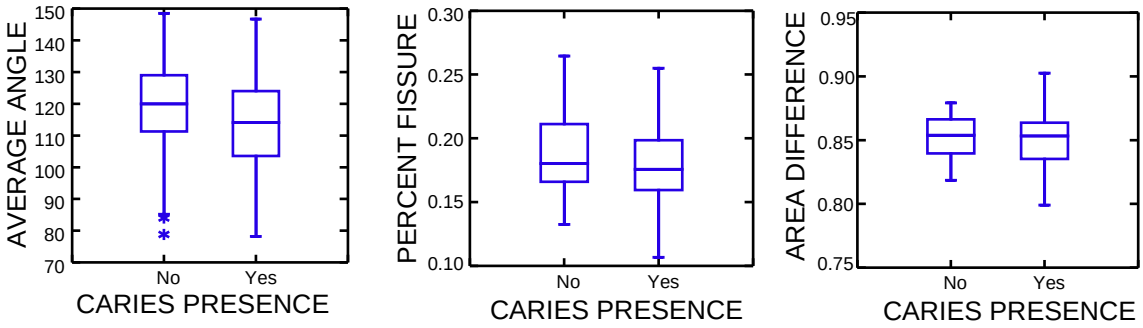

Figure 8. Variation in initial caries presence or absence based on the three fissure attributes.

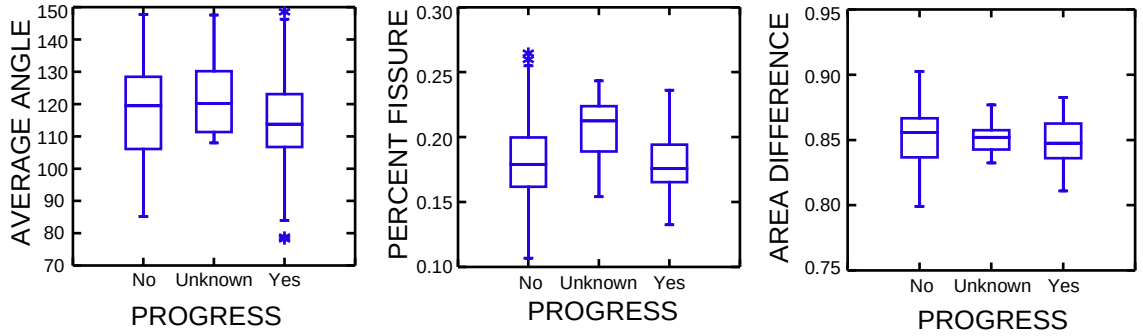

Figure 9. Variation in caries progression from initial to final scoring based on the three fissure attributes. (Unknown=teeth that were restored or sealed in the final examination.)

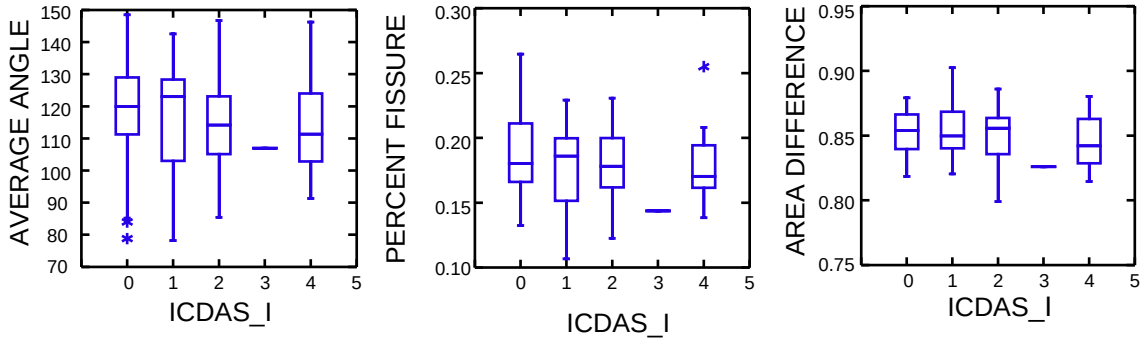

Figure 10. Variation in initial ICDAS scores based on the three attributes. (There were no specimens scored higher than a 4.)

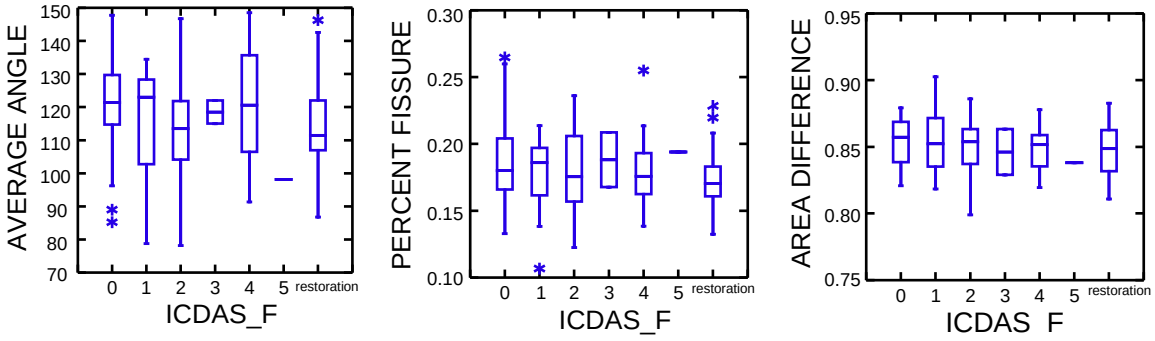

Figure 11. Variation in final ICDAS scores based on the three attributes. (There were no specimens scored higher than a 5.)

Spearman Correlation Matrix

	AVG	AREA_DIF	PERC_FISSURE
AVG	1		
AREA_DIF	0.220 (p=0.004399)	1	
PERC_FISSURE	0.341 (p<0.00001)	-0.267 (p=0.000506)	1

Table 5. Spearman's Correlation Coefficients (r_s) among the three quantified fissure attributes.

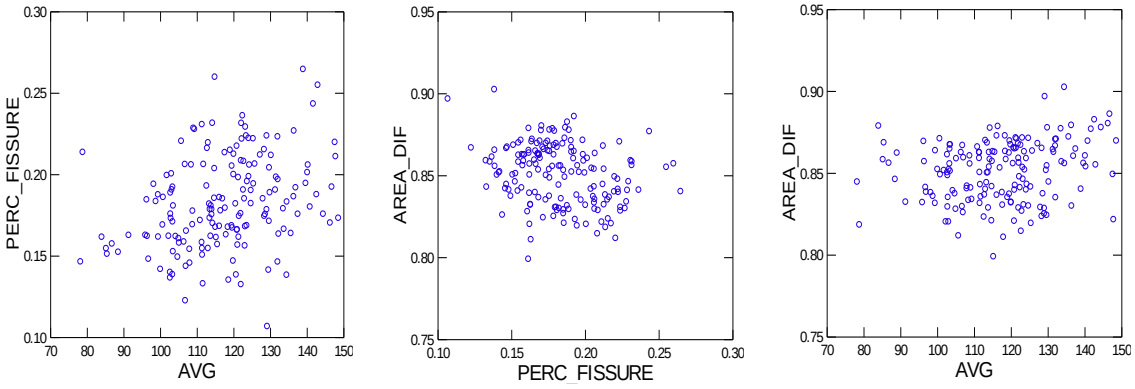

Figure 12. Bivariate plots comparing fissure attributes among specimens considered.